Dalton Transactions

COMMUNICATION

View Article Online
View Journal | View Issue

Cite this: *Dalton Trans.*, 2016, **45**, 494

Received 12th November 2015,
Accepted 19th November 2015

DOI: 10.1039/c5dt04470g

www.rsc.org/dalton

A luminescent europium(III)–platinum(II) heterometallic complex as a theranostic agent: a proof-of-concept study†‡

Anirban Chandra,§[a] Khushbu Singh,§[a] Swati Singh,[b] Sri Sivakumar[b] and Ashis K. Patra*[a]

A luminescent heterometallic multifunctional theranostic Eu–Pt_2 complex [{*cis*-$PtCl_2$(DMSO)}$_2$Eu(L)(H_2O)] has been synthesized, possessing two therapeutic Pt-centers as covalent DNA binders and one emissive Eu^{3+}-center which is sensitized by platinum-based metal-to-ligand charge-transfer excited states.

Multifunctional cancer theranostic agents with multiple therapeutic and diagnostic centers in a single platform have gained popularity in recent years.[1–3] Recently, there are a few reports on heterometallic hairpin-shaped lanthanide–Pt_2 complexes for DNA recognition and magnetic resonance imaging (MRI) based theranostic agents or for selectively delivering gadolinium to tumor cell nuclei.[4] In this regard, theranostic Gd^{3+}-based platinum complexes have been reported[4c] in which Gd^{3+} and conjugated *cis*-$[Pt(NH_3)_2Cl]^+$-moieties act as MRI contrast and therapeutic centers, respectively. These complexes showed therapeutic efficiency along with improved MR imaging capability. However, their DNA-binding ability is limited because there are only two available DNA-crosslinking sites. In addition, the clinical use of platinum drugs is severely affected by drug resistance mediated by inadequate levels of platinum reaching critical target DNA.[5] Notwithstanding this progress, it is highly desirable to increase the DNA binding sites that significantly enhance platinum content at target sites along with the tagging of a bright luminescent center as a diagnostic probe. To this end, we report the design of a multimodal targeted theranostic Eu–Pt_2 conjugate possessing four DNA binding sites which can effectively target nuclear DNA along with a highly luminescent Eu^{3+} center to enable interference-free live-tracking of the drug using fluorescence microscopy. Luminescent lanthanide complexes were widely exploited in various bioassays since they offer unique photophysical properties like narrow emission bands, a large Stokes' shift and long-lived excited state lifetimes.[6,7] Since direct excitation of a Ln^{3+} f–f transition is very inefficient, chemists have designed a variety of chelating agents conjugated to a sensitizing organic chromophore called an *antenna*, which can transfer its excited state energy efficiently to the emissive Ln^{3+} ion leading to bright luminescence compared to the direct excitation of Ln^{3+} ions.[8,9] Our approach exploits the advantages of transition metal complexes as they exhibit many desirable properties as a sensitizer than as an organic chromophore, such as tunable absorption bands, long-lived excited states which maximize the ET to Ln^{3+}, excellent photochemical stability and kinetic inertness.[10,11]

Herein, we demonstrate a multifunctional Eu–Pt_2 complex, [{*cis*-$PtCl_2$(DMSO)}$_2$Eu(L)(H_2O)] (**1**) (Scheme 1), which has cytotoxic *cis*-$[PtCl_2(DMSO)]$ moieties that enable DNA binding, whereas the EuL unit acts as a luminescent reporter. Thus, a combination of a luminescent imaging probe and a conju-

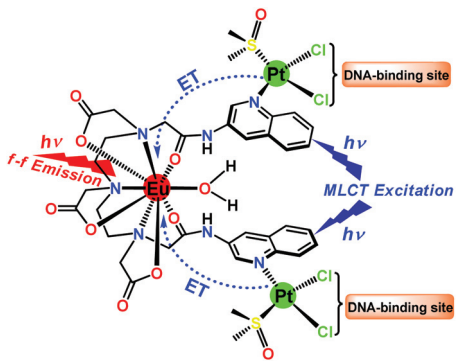

Scheme 1 Molecular structure of Eu–Pt_2 complex **1** showing a Pt → Eu energy transfer pathway upon MLCT photo-excitation leading to f–f emission from Eu^{3+} and dissociable Pt–Cl bonds as DNA-cross linking sites.

[a]*Department of Chemistry, Indian Institute of Technology Kanpur, Kanpur 208016, Uttar Pradesh, India. E-mail: akpatra@iitk.ac.in*
[b]*Department of Chemical Engineering and Centre for Environmental Science and Engineering, Indian Institute of Technology Kanpur, Kanpur-208016, U.P., India*

†Dedicated to Professor Animesh Chakravorty on the occasion of his 80th birthday.

‡Electronic supplementary information (ESI) available: Experimental details; synthesis and characterization of compounds; ESI-MS analysis; DNA and BSA binding experiments; cytotoxicity and cellular internalization studies. See DOI: 10.1039/c5dt04470g

§A. C. and K. S. contributed equally to this work.

gated therapeutic agent in a single hybrid 5d–4f complex can provide real-time feedback on drug delivery, distribution and target site localization in a non-invasive manner using fluorescence microscopy. Another key design feature of this complex is having four potential DNA cross-linking sites due to the presence of labile Pt–Cl bonds, thus a higher level of activated platinum will reach DNA, which is a possible way to lower drug resistance. Eu–Pt_2 complex **1** was prepared in a sequential manner (Scheme S1, ESI‡) starting with a multidentate DTPA-bisamide ligand, H_3L = *N*,*N*″-bis(3-amidoquinolyl) diethylenetriamine-*N*,*N*′,*N*″-triacetic acid, derived from the acylation of 3-aminoquinoline by DTPA-bis(anhydride). [Eu(L)(H_2O)] was synthesized by reacting a 1 : 1 molar ratio of the deprotonated ligand and $Eu(NO_3)_3{\cdot}6H_2O$ in water. [{*cis*-$PtCl_2(DMSO)\}_2$Eu(L)(H_2O)] (**1**) was isolated after the reaction of EuL with freshly prepared *cis*-[$Pt(DMSO)_2Cl_2$] in a 1 : 2 molar ratio. Detailed ESI-MS studies of the Eu–Pt_2 complex reveal an *m*/*z* of 714.52 corresponding to $\{M - 2Cl\}^{2+}$ with a matching isotopic distribution profile, which can be unequivocally attributed to the formation of Eu–Pt_2 along with other physicochemical data (Fig. S1, ESI‡). We observed dissociable chloride ligands in aqueous solution which is crucial for forming cross-links with base pairs in nuclear DNA.

The UV-vis spectrum of **1** exhibits a high energy band at 273 nm due to ligand centered $\pi \rightarrow \pi^*$ transitions and a broad band ranging from 332–350 nm corresponding to $\pi \rightarrow \pi^*$ MLCT transitions of the quinoline bound Pt^{2+} moiety (Fig. 1a). Here we have judiciously utilized this ^{3}MLCT excited state as a means to populate the $^5D_0$ emissive states of europium through efficient energy transfer. The ^{3}MLCT → *f* energy transfer through such photosensitization is shown in few Eu–Pt complexes.[12] The addition of *cis*-[$Pt(DMSO)_2Cl_2$] to EuL resulted in the appearance of a new band at 350 nm with an isobestic point at ~270 nm, indicative of the formation of Eu–Pt_2 complex **1** during titration (Fig. S2 in ESI‡). Upon excitation of the MLCT band, the Eu–Pt_2 complex under time-gated mode displayed narrow emission bands spanning from 575–700 nm characteristic of the $^5D_0 \rightarrow {}^7F_J$ (J = 0–4) f–f transitions of Eu^{3+} (Fig. 1b). The luminescence spectra demonstrate the efficient photosensitized energy transfer from the MLCT excited state of the quinoline bound Pt^{2+} moiety to the emissive $^5D_0$ excited state of Eu^{3+} with an overall quantum yield ($\phi_{overall}$) of 0.04. Spectrophotometric titration of *cis*-[$Pt(DMSO)_2Cl_2$] with [Eu(L)(H_2O)] at λ_{ex} = 330 nm showed the formation of [{*cis*-$PtCl_2(DMSO)\}_2$Eu(L)(H_2O)] (**1**) with a gradual increase in europium centered emission until it reached a plateau at Eu/Pt = 0.5 (Fig. 1c). The decay rate of the emissive $^5D_0$ excited state measured at 616 nm results in a monoexponential decay curve with a lifetime (τ_{obs}) of 0.65(±10%) ms in aqueous buffer medium, indicating the presence of a single chemical environment. The enhancement of the τ_{obs} in the presence of DNA (τ_{obs} = 0.89 (±10%) ms) indicates minimization of the nonradiative relaxation pathways in the DNA bound form of the Eu–Pt_2 complex (Fig. 1d).

Since DNA is the most important target for therapeutic platinum drugs, we attempted detailed binding studies of **1** with DNA. The hairpin-shaped complex **1** is activated by aquation through the substitution of the chloride ligands by water which generates a potent cation, [Eu(L)(H_2O)\{*cis*-$Pt(OH_2)_{n/2}(DMSO)\}_2]^{n+}$ (n = 1–4), which can readily cross-link with the nucleobases of ds-DNA (Scheme S2, ESI‡). The binding interaction of the Eu–Pt_2 complex with calf-thymus DNA (CT-DNA) was studied using UV-vis titration, competitive displacement of ethidium bromide by fluorescence (K_{app} = 4.9 × 10^5 M^{-1}), circular dichroism (CD) and isothermal titration calorimetry (ITC) (Fig. S6–S8, ESI‡). The ITC titration plot suggests a biphasic sequential binding interaction[13] of Eu–Pt_2 with CT-DNA with an initial favorable exothermic binding event (K_1 = 1.7 × 10^5 M^{-1}, ΔH_1 = −26.0 kcal mol^{-1}), followed by a second exothermic event (K_2 = 9.1 × 10^5 M^{-1}, ΔH_2 = −77.6 kcal mol^{-1}) presumably due to successive sequential covalent cross-link formation with base pairs of duplex-DNA (Fig. 2a). The intrinsic binding constant (K_b = 1.5(±0.3) × 10^5 M^{-1}) along with a hypochromism and bathochromic shift of the electronic spectral bands suggests a favorable binding interaction of the complex **1** with DNA due to $EuPt_2$–DNA adduct formation, strong electrostatic interaction with activated $\{Eu\text{–}Pt_2\}^{n+}$ and favorable stacking interactions of the two planar –Pt(L) chromophores with the planar base pairs of ds-DNA as observed in similar hairpin shaped Eu–Pt_2 complexes.[4a,b] Formation of such bis(bifunctional) platinum-DNA cross-links should induce major unrepairable structural distortion of the DNA double-helix. The significant decrease in ellipticity in the CD spectra of CT-DNA in the presence of **1** (Fig. 2b) also suggests unwinding of the DNA helix and major structural deformation of DNA induced by the Pt–DNA cross-links.[14] This structural

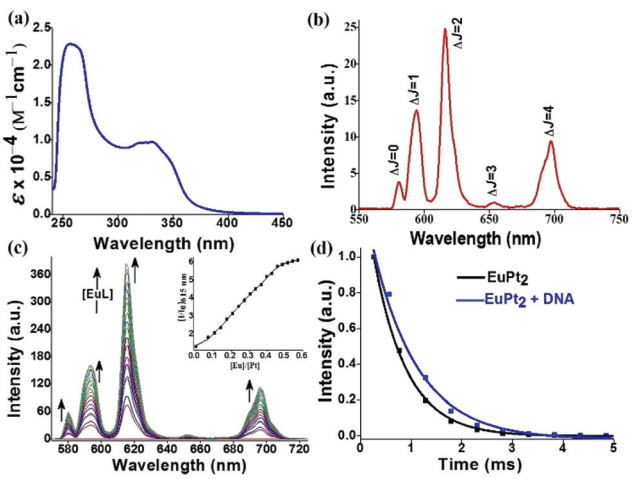

Fig. 1 (a) UV-vis and (b) emission spectrum (λ_{ex} = 330 nm) of Eu–Pt_2 complex **1** in Tris-HCl buffer. (c) Evolution of the emission spectra with increasing [EuL] added to a solution of [$PtCl_2(DMSO)_2$] in DMF (λ_{ex} = 330 nm), Inset: the plot of relative emission intensity at 615 nm *vs*. [Eu]/[Pt] ratio. (d) Luminescence decay profile from the $^5D_0$ state of Eu^{3+} in complex **1** at λ_{em} = 616 nm (λ_{ex} = 330 nm) (black) and in the presence of CT-DNA (blue) in Tris-HCl buffer (pH = 7.2). [**1**] = 90 μM, [DNA] = 450 μM, delay time and gate time = 0.1 ms. The solid lines are the best fits considering the single-exponential behaviour of the decay.

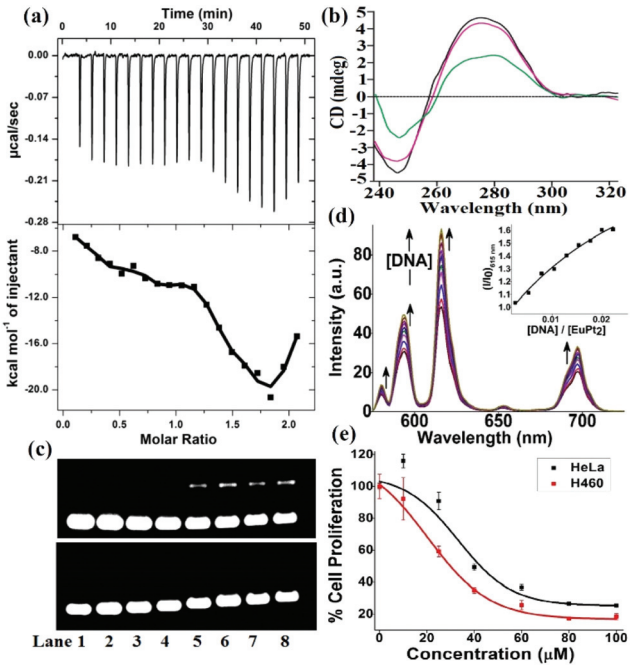

Fig. 2 (a) ITC plot profile for the interaction of Eu–Pt_2 (0.1 mM) with CT-DNA (0.01 mM) in 5 mM Tris-HCl/NaCl buffer (pH 8.5) at 30 °C. The top panel represents the raw data for 20 injections of 2 µL each. The bottom panel shows the amounts of heat evolved on interaction of the Eu–Pt_2 complex with CT-DNA against the molar ratio of Eu–Pt_2 complex to CT-DNA. Data were fitted by a sequential binding site model. (b) CD spectra of CT-DNA in the presence of EuL and Eu–Pt_2 in Tris-HCl buffer medium. (c) Agarose gel electrophoresis of SC pUC19 DNA after incubation with EuL and Eu–Pt_2 in 50 mM Tris-HCl buffer at 37 °C for 16 h. Lane 1: DNA control, lanes 2–8 (10, 15, 20, 40, 60, 80 and 100 µM complexes respectively). (d) Luminescence spectra of Eu–Pt_2 (λ_{ex} = 330 nm) with the addition of CT-DNA in 5 mM Tris-HCl buffer. Inset: the relative emission intensity (I/I_0) of **1** at 615 nm *vs.* [DNA]/[Eu–Pt_2] ratio. (e) Cell viability plots showing the cytotoxicity of the Eu–Pt_2 complex with HeLa and H460 cells on 16 h incubation by MTT assay.

distortion of DNA could be beyond cellular DNA repair machinery and thereby inhibit transcription and replication, triggering cell-death pathways.[5] The decrease in DNA migration rate in the presence of Eu–Pt_2 compared to EuL in the gel electrophoretic mobility assay using SC pUC19 DNA also suggests unwinding of the supercoiled DNA helix by **1** (Fig. 2c).[15] We have observed significant enhancement of the Eu-based luminescence intensity originating from the $^5D_0 \rightarrow {}^7F_J$ transitions of Eu^{3+} upon the addition of DNA due to efficient energy transfer to Eu^{3+} and enhanced excited state lifetime in a hydrophobic environment created due to binding of the Eu–Pt_2 complex with DNA (Fig. 2d). Serum albumin proteins constitute a major component in blood plasma proteins and play important roles in drug transport and metabolism. The interaction of the Eu–Pt_2 complex with bovine serum albumin (BSA) studied using a tryptophan emission quenching experiment showed a high binding propensity (K_{BSA} = 1.50 ± 0.03 × 10^5 M^{-1}) desirable for efficient transport to the pathological site (Fig. S9, ESI‡).

To test our original '*theranostic*' design, we performed an *in vitro* cytotoxicity assay using MTT on human cervical carcinoma HeLa and lung carcinoma H460 cell lines. The IC_{50} values for Eu–Pt_2 complex **1** are 51.0 ± 1.05 µM in HeLa cells and 30.0 ± 1.27 µM in H460 cells (Fig. 2d). It exerts anticancer activity *via* extensive DNA-adduct formation through conjugated *cis*-[$PtCl_2$(DMSO)] moieties with a similar mechanism to cisplatin.

The cellular internalization of the Eu–Pt_2 complex was investigated to probe the diagnostic aspect of [Eu(L)(H_2O)] utilizing the long luminescence lifetime and intrinsic luminescence from Eu^{3+} using confocal fluorescence microscopy (panel A, Fig. 3). The theranostic Eu–Pt_2 complex showed significant cellular uptake within 4 h of incubation with the HeLa cells. Staining with nuclear staining dye Hoechst 33258 demonstrates both nuclear and cytosolic distribution of the complex (panel C, Fig. 3). The red spots observed in some nuclei originate from the luminescence of the Eu^{3+} reporter tag in the Eu–Pt_2 theranostic conjugate (Fig. S11, ESI‡).

In conclusion, we have developed a luminescent multimodal heterometallic Eu–Pt_2 theranostic system using sensitization and energy transfer from a conjugated Pt^{2+} based chromophore to Eu^{3+}. The complex shows a strong binding propensity for DNA *via* the formation of Pt–DNA cross-links through four potential DNA binding sites. The complex exhibits cytotoxicity through DNA damage, and nuclear localization due to an Eu-based f–f transition is observed using fluorescence imaging. Thus, such systems will have great

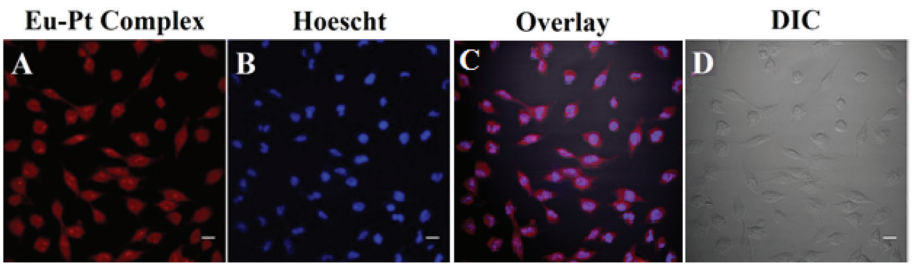

Fig. 3 Confocal laser scanning fluorescence microscopic images of the HeLa cells treated with the Eu–Pt_2 complex (25 µM) after 4 h of incubation and Hoechst 33258 dye (5 µg mL^{-1}): (A) cells incubated with the Eu–Pt_2 complex; (B) incubated with the Hoechst 33258 dye for staining nuclei, which show blue emission; (C) merged images showing nuclear and cytosolic localization of the complex; (D) DIC images. Scale bar = 20 µm.

potential towards designing theranostic agents and delivery vehicles for cancer chemotherapy. Further studies are ongoing towards designing potent lanthanide based theranostic agents as efficient drug delivery platforms and understanding the mechanism of their action.

A.K.P. acknowledges SERB, Govt. of India and IIT Kanpur for funding. A.C. and K.S. acknowledge UGC and CSIR for their research fellowships.

Notes and references

1 (*a*) H. Koo, M. S. Huh, I.-C. Sun, S. H. Yuk, K. Choi, K. Kim and I. C. Kwon, *Acc. Chem. Res.*, 2011, **44**, 1018–1028; (*b*) T. Lammers, S. Aime, W. E. Hennink, G. Storm and F. Kiessling, *Acc. Chem. Res.*, 2011, **44**, 1029–1038.

2 (*a*) M. K. Yu, J. Park and S. Jon, *Theranostics*, 2012, **2**, 3–44; (*b*) J. D. Rocca, D. Liu and W. Lin, *Acc. Chem. Res.*, 2011, **44**, 957–968; (*c*) M. Liong, J. Lu, M. Kovochich, T. Xia, S. G. Ruehm, A. E. Nel, F. Tamanoi and J. I. Zink, *ACS Nano*, 2008, **2**, 889–896.

3 A. S. Paraskar, S. Soni, K. T. Chin, P. Chaudhuri, K. W. Muto, J. Berkowitz, M. W. Handlogten, N. J. Alves, B. Bilgicer, D. M. Dinulescu, R. A. Mashelkar and S. Sengupta, *Proc. Natl. Acad. Sci. U. S. A.*, 2010, **107**, 12335–12340.

4 (*a*) P. B. Glover, P. R. Ashton, L. J. Childs, A. Rodger, M. Kercher, R. M. Williams, L. D. Cola and Z. Pikramenou, *J. Am. Chem. Soc.*, 2003, **125**, 9918–9919; (*b*) E. L. Crossley, J. B. Aitken, S. Vogt, H. H. Harris and L. M. Rendina, *Angew. Chem., Int. Ed.*, 2010, **49**, 1231–1233; (*c*) Z. Zhu, X. Wang, T. Li, S. Aime, P. J. Sadler and Z. Guo, *Angew. Chem., Int. Ed.*, 2014, **53**, 13225–13228; (*d*) H. Li, R. Lan, C.-F. Chan, L. Jiang, L. Dai, D. W. J. Kwong, M. H.-W. Lam and K.-L. Wong, *Chem. Commun.*, 2015, **51**, 14022–14025.

5 (*a*) D. Wang and S. J. Lippard, *Nat. Rev. Drug Discovery*, 2005, **4**, 307–320; (*b*) L. Kelland, *Nat. Rev. Cancer*, 2007, **7**, 573–584.

6 S. Cotton, *Lanthanides and actinides*, McMillan Physical Science Series, McMillan Education, London, 1991.

7 (*a*) J.-C. G. Bünzli, *Chem. Rev.*, 2010, **110**, 2729–2755; (*b*) J.-C. G. Bünzli and S. V. Eliseeva, *Chem. Sci.*, 2013, **4**, 1939–1949; (*c*) E. J. New, A. Congreve and D. Parker, *Chem. Sci.*, 2010, **1**, 111–118; (*d*) E. J. New, D. Parker, D. G. Smith and J. W. Walton, *Curr. Opin. Chem. Biol.*, 2010, **14**, 238–246.

8 (*a*) M. C. Heffern, L. M. Matosziuk and T. J. Meade, *Chem. Rev.*, 2014, **114**, 4496; (*b*) A. J. Amoroso and S. J. A. Pope, *Chem. Soc. Rev.*, 2015, **44**, 4723–4772; (*c*) S. J. Butler, M. Delbianco, L. Lamarque, B. K. McMahon, E. R. Neil, R. Pal, D. Parker, J. W. Walto and J. M. Zwier, *Dalton Trans.*, 2015, **44**, 4791–4803.

9 X. Wang, H. Chang, J. Xie, B. Zhaoa, B. Liu, S. Xu, W. Pei, N. Ren, L. Huang and W. Huang, *Coord. Chem. Rev.*, 2014, **273/274**, 201–212.

10 (*a*) S. Faulkner, L. S. Natarajan, W. S. Perry and D. Sykes, *Dalton Trans.*, 2009, 3890–3899; (*b*) M. D. Ward, *Coord. Chem. Rev.*, 2010, **254**, 2634–2642; (*c*) F.-F. Chen, Z.-Q. Chen, Z.-Q. Bian and C.-H. Huang, *Coord. Chem. Rev.*, 2010, **254**, 972–990.

11 (*a*) S. I. Klink, H. Keizer and F. C. J. M. van Veggel, *Angew. Chem., Int. Ed.*, 2000, **39**, 4319–4321; (*b*) S. J. A. Pope, B. J. Coe, S. Faulkner, E. V. Bichenkova, X. Yu and K. D. Douglas, *J. Am. Chem. Soc.*, 2004, **126**, 9490–9491; (*c*) E. Baggaley, D.-K. Cao, D. Sykes, S. W. Botchway, J. A. Weinstein and M. D. Ward, *Chem. – Eur. J.*, 2014, **20**, 8898–8903.

12 (*a*) P. Kadjane, C. P.-Iglesias, R. Ziessel and L. J. Charbonnière, *Dalton Trans.*, 2009, 5688–5700; (*b*) R. Ziessel, S. Diring, P. Kadjane, L. Charbonnière, P. Retailleau and C. Philouze, *Chem. – Asian J.*, 2007, **2**, 975–982; (*c*) T. K. Ronson, T. Lazarides, H. Adams, S. J. A. Pope, D. Sykes, S. Faulkner, S. J. Coles, M. B. Hursthouse, W. Clegg, R. W. Harrington and M. J. Ward, *Chem. – Eur. J.*, 2006, **12**, 9299–9313.

13 (*a*) N. Inukai, T. Kawai and J. Yuasa, *Chem. – Eur. J.*, 2013, **19**, 5938–5947; (*b*) N. Inukai, T. Kawai and J. Yuasa, *Chem. Commun.*, 2011, **47**, 9128–9130; (*c*) J. Yuasa, T. Ohno, H. Tsumatori, R. Shiba, H. Kamikubo, M. Kataoka, Y. Hasegawa and T. Kawai, *Chem. Commun.*, 2013, **49**, 4604–4606; (*d*) C. P. Montgomery, E. J. New, D. Parker and R. D. Peacock, *Chem. Commun.*, 2008, 4261–4263.

14 W. C. Johnson, *Circular Dichroism: Principles and Applications*, ed. K. Nakanishi, N. Berova and R. W. Woody, VCH, New York, 1994, pp. 523–540.

15 M. V. Keck and S. J. Lippard, *J. Am. Chem. Soc.*, 1992, **114**, 3386–3390.